Prepared for submission to JINST

4TH International Conference Frontiers in Diagnostic Technologies
30 March 2016 - 01 April 2016
Frascati, Italy

Importance of energy and angular resolutions in top-hat electrostatic analysers for solar wind proton measurements

R. De Marco,[a,1] **M.F. Marcucci,**[a] **R. Bruno,**[a] **R. D'Amicis,**[a] **S. Servidio,**[b] **F. Valentini,**[b] **B. Lavraud,**[c,d] **P. Louarn,**[c,d] **M. Salatti**[e]

[a] *INAF-Istituto di Fisica e Planetologia Spaziali, Via del Fosso del Cavaliere 100, 00133 Roma, Italy*

[b] *Dipartimento di Fisica, Università della Calabria, I-87030 Rende (CS), Italy*

[c] *Institut de Recherche en Astrophysique et Planétologie, Université de Toulouse, France*

[d] *Centre National de la Recherche Scientifique, UMR 5277, Toulouse, France*

[e] *Agenzia Spaziale Italiana, Via del Politecnico snc, 00133 Roma, Italy*

E-mail: rossana.demarco@iaps.inaf.it

Abstract: We use a numerical code which reproduces the angular/energy response of a typical top-hat electrostatic analyser starting from solar wind proton velocity distribution functions (VDFs) generated by numerical simulations. The simulations are based on the Hybrid Vlasov-Maxwell numerical algorithm which integrates the Vlasov equation for the ion distribution function, while the electrons are treated as a fluid. A virtual satellite launched through the simulation box measures the particle VDFs. Such VDFs are moved from the simulation Cartesian grid to energy-angular coordinates to mimic the response of a real sensor in the solar wind. Different energy-angular resolutions of the analyser are investigated in order to understand the influence of the phase-space resolution in existing and upcoming space missions, with regards to determining key parameters of plasma dynamics.

Keywords: Particle detectors, Instrument optimisation

[1] Corresponding author.

Contents

1 Introduction

The Universe is permeated by hot, turbulent magnetized plasmas. Energy injected in the system by large scales phenomena, such as shear motions, shock waves, jets, is transferred with negligible dissipation to smaller and smaller scales by the so-called energy turbulent cascade. Dissipation takes place at kinetic scales, where the scales of the turbulent fluctuations become comparable with the typical particles scales, e.g. gyroradii. A variety of fluctuations operate at these scales in collisionless plasmas which are associated to different heating and acceleration mechanisms, like wave generation and damping, instabilities, magnetic reconnection.

This aspect has been unexplored from an observational point of view due to the lack of dedicated plasma measurements. In the recent years, a better understanding of energy dissipation mechanisms and particle energization has been achieved thanks to direct numerical simulations. Vlasov [1, 2], hybrid [3] and Particle-In-Cell [4–6] codes are able to reproduce the features of the modified particle distribution functions as a consequence of particle energization. Yet, numerical simulations may deal only with specific scales and particle species at a time, while studying energy dissipation require resolving simultaneously the different typical scales of all the particles involved: electrons, protons and heavy ions.

In the near future, *in situ* instrumentation onboard the missions THOR and Solar Orbiter will provide important measurements to study the fundamental link between turbulence, energy dissipation and particle energization. Turbulence Heating ObserveR (THOR), candidate as next ESA M4 mission, to be launched if selected in 2026, is the first mission entirely devoted to the study of space turbulence, and would be the first satellite ever tailored to perform field and particle measurements at kinetic scales in different near-Earth regions and in the solar wind. Solar Orbiter (SolO), together with Solar Probe Plus, to be launched in 2018, will be the first spacecraft since Helios to sample the inner heliosphere inside the orbit of Mercury, and will provide comprehensive remote and *in situ* measurements which are critical to establish the fundamental physical links between the Sun's dynamic atmosphere and the turbulent solar wind.

THOR and Solar Orbiter, due to their different orbits would allow to compare and address the important question of turbulence evolution as a function of the distance from the Sun and will provide unprecedented measurements to study the fundamental processes related to particle heating and acceleration mechanisms.

2 Particle measurements in space

Measurements of particle velocity distribution functions (VDF) are of primary importance in plasma physics. These kinds of measurements are tipically performed by top-hat electrostatic analysers [7]. These instruments will be onboard of both Solar Orbiter and THOR. A top-hat analyser (a schematic illustration of the instrument is given in figure 1) is made of two concentric hemispheres

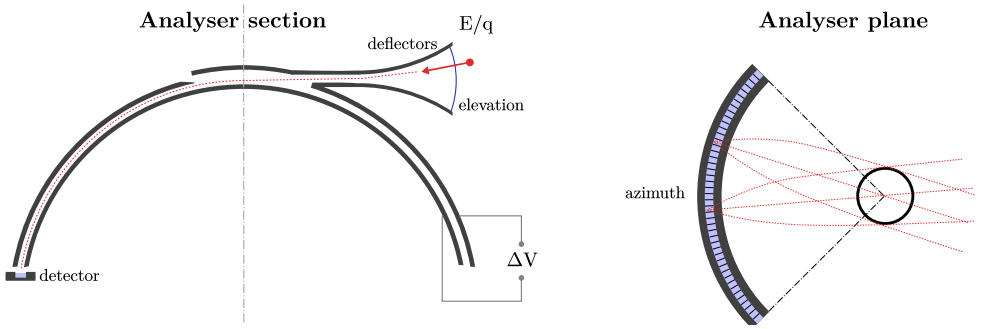

Figure 1. Cross-section and top views of a top-hat analyser for the observation of the solar wind, with a sketch of its focusing properties.

set at different voltage, with an aperture on the outer hemisphere. The electric field existing between the plates allows for particles within a specific energy-per-charge (E/q) ratio to pass through the aperture and through the gap between the plates. Parallel incident particles will be focused in a small spot on the detector plane, which is partitioned in sectors. Full coverage of the entire 4π solid angle can be obtained by rotating the analyser (i.e. on a spinning spacecraft) or by using multiple sensor heads equipped with electrostatic polar expansions which select the angle of incident particles direction. In this way a top-hat analyser provides the distribution of particles in spherical coordinates in velocity space. The response of an electrostatic analyser with a given angular and energy resolution depends on its own geometric factor.

To resolve the kinetic scales a high resolution in energy, angle and time is required. Yet building up instruments with such high capability may be extremely demanding. Therefore it is crucial to find the right tradeoff between scientifical requirements and technical restrictions.

3 Importance of phase space resolution

Numerical simulations of solar wind turbulence show that kinetic effects manifest as evident non-Maxwellian shapes of the distribution functions such as anisotropies or beams [8–10]. Moreover heating occours close to regions where thin current sheets are produced through the turbulent cascade [11]. The energy-angular resolution of the particle instruments is crucial for the observation of these fine structures, which would be smoothed out if a sampling of VDFs over low resolution

phase space or long times is done. To assess how the smallest features of the ion VDFs resulting from a numerical simulation would be detected by a particle sensor of top-hat type, we consider two top-hat analysers dedicated to the study of solar wind: Proton Alpha Sensor, onboard Solar Orbiter, and Cold Solar Wind [12, 13] onboard THOR. PAS has 9 elevation angles of 5° degrees and 11 azimuthal sectors, 6° degrees each, so with a field of view of 45° × 66° degrees. The energy sweep has 96 bins and a $\Delta E/E = 4.80\%$, the geometric factor is $G = 4.6 \times 10^{-6}\text{cm}^2\text{sr}$ and the acquisition time is $T_{acc} = 0.96\text{ms}$. For CSW (currently in the study phase) we consider 64 energy intervals, $\Delta E/E = 7\%$, a field of view of 48° both in elevation and azimuth and two different angular resolutions: the first one, which we will refer as Low Resolution (CSW-LR) has 16 angles in elevation and azimuth, a geometric factor per anode $G = 4.4 \times 10^{-5}\text{cm}^2\text{sr}$ and an accumulation time $T_{acc} = 0.5\text{ms}$. The second configuration, the High Resolution one (CSW-HR) has 32 angles in elevation and azimuth, a geometric factor $G = 2.2 \times 10^{-5}\text{cm}^2\text{sr}$ and an accumulation time $T_{acc} = 0.25\text{ms}$. These instruments have a restricted field of view and a high angular resolution since they are designed to sample the solar wind, which is a cold and focused beam in velocity space.

As a starting point we use the VDFs resulting from a Hybrid Vlasov-Maxwell (HVM) simulation of the turbulent solar wind, which solves the Vlasov equation for protons while electrons are considered as a fluid, along with Maxwell equations for electromagnetic fields (see [11] for simulation details). The initial Maxwellian ion VDF is perturbed by a 2D spectrum of fluctuations for the magnetic and velocity fields, and the turbulent Vlasov cascade is let to evolve. At a given time, a cut is made in physical space and 1024 VDFs are collected in a solar wind-like sampling. These VDFs are reconstructed in the field of view of the sensors (by an averaging process), then we compute the counts that the sensors would see in each energy-angular bin, as [7]:

$$\text{counts}_{i,j,k} = v_i^4 \cdot f_{i,j,k} \cdot T_{acc} \cdot G \tag{3.1}$$

where i, j, k refer to the energy, elevation and azimuth intervals, v_i is the velocity in the interval, f the distribution function, T_{acc} and G the accumulation time and the geometric factor respectively. It is worth noting that, even if we start from the same distribution functions, each sensor sees a different number of counts, due to its own sensitivity and geometrical features. Afterwards, using a *top-hat simulator* we compute moments and the VDFs as sampled by the sensors.

As representative examples we report, in figures 2 and 3, two VDFs as they look like from the HVM simulation, and how they will be sampled by the three sensor configurations: CSW-LR, CSW-HR and PAS. The first VDF is characterized by strong anisotropy as well as ring-like features. These rings are still well recognizable in CSW-HR, while they fade away in CSW-LR and are completely lost in PAS. The second VDF is characterized by a second population of particles along the local magnetic field and ring-like structures. As before, CSW-HR performs better in reproducing the features of the original VDF while for PAS, due to the lower phase space resolution, this suprathermal component is not clearly detached from the core of the distribution.

4 Moments calculations

In order to assess the effects of phase space resolution in the moments of the distribution functions we computed the density, the three components of velocities and the temperatures parallel and

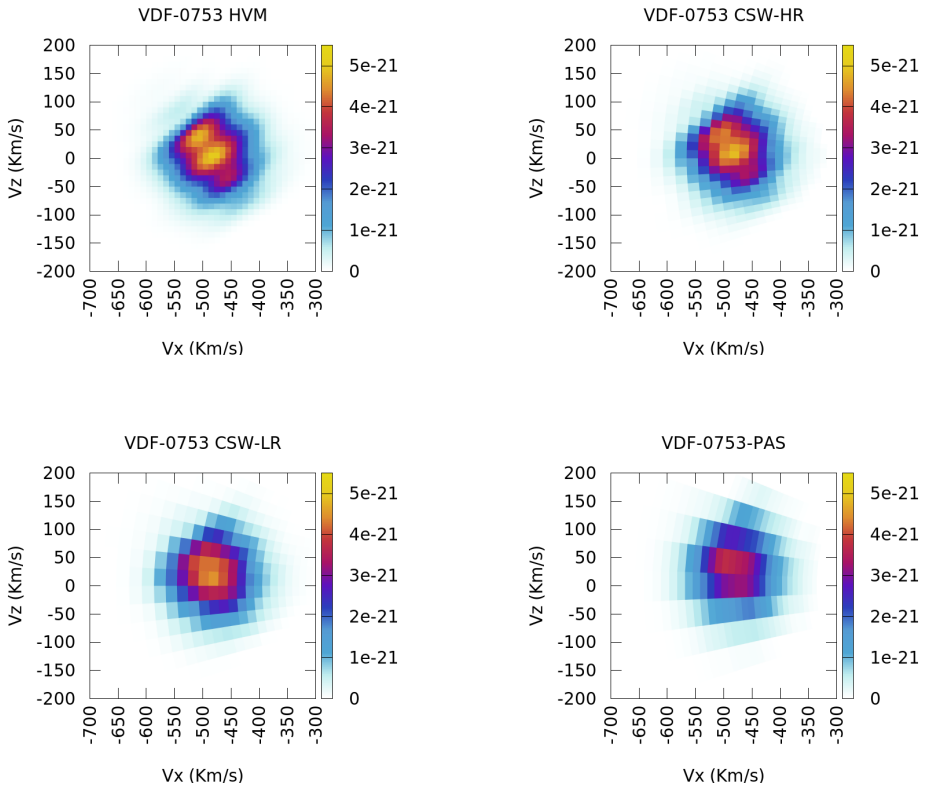

Figure 2. VDF # 1 (in $cm^{-6}s^3$) as it appears from the HVM simulation (top left), and as it would appear from the CSW detectors (top right and bottom left) and from PAS (bottom right).

perpendicular to the local magnetic field for the 1024 VDFs. The plasma density is given by:

$$n((\mathbf{r},t) = \int f(\mathbf{r},\mathbf{v},t)d^3\mathbf{v}. \tag{4.1}$$

The bulk velocity vector is given by:

$$V_i(\mathbf{r},t) = \frac{1}{n}\int v_i f(\mathbf{r},\mathbf{v},t)d^3\mathbf{v}, \tag{4.2}$$

where n is the density, and temperature is obtained from the pressure tensor components, defined as:

$$P_{ij}(\mathbf{r},t) = m\int (v_i - V_i)\cdot(v_j - V_j)f(\mathbf{r},\mathbf{v},t)d^3\mathbf{v}. \tag{4.3}$$

given that $\mathbf{P} = nk\mathbf{T}$ (k being the Boltzmann constant). We calculate the moments using the simulated sensors and compare them with those obtained from the HVM simulation. Results show that different resolutions have small effects on moments, especially in density and velocity (see figure 4 top and middle panels). Temperature is more affected, especially for PAS, as shown in the bottom panel of figure 4 (only total temperature is reported). The temperature anisotropy $A = T_\perp/T_\parallel$ doesn't seem to depend on the three different sensors (figure 5).

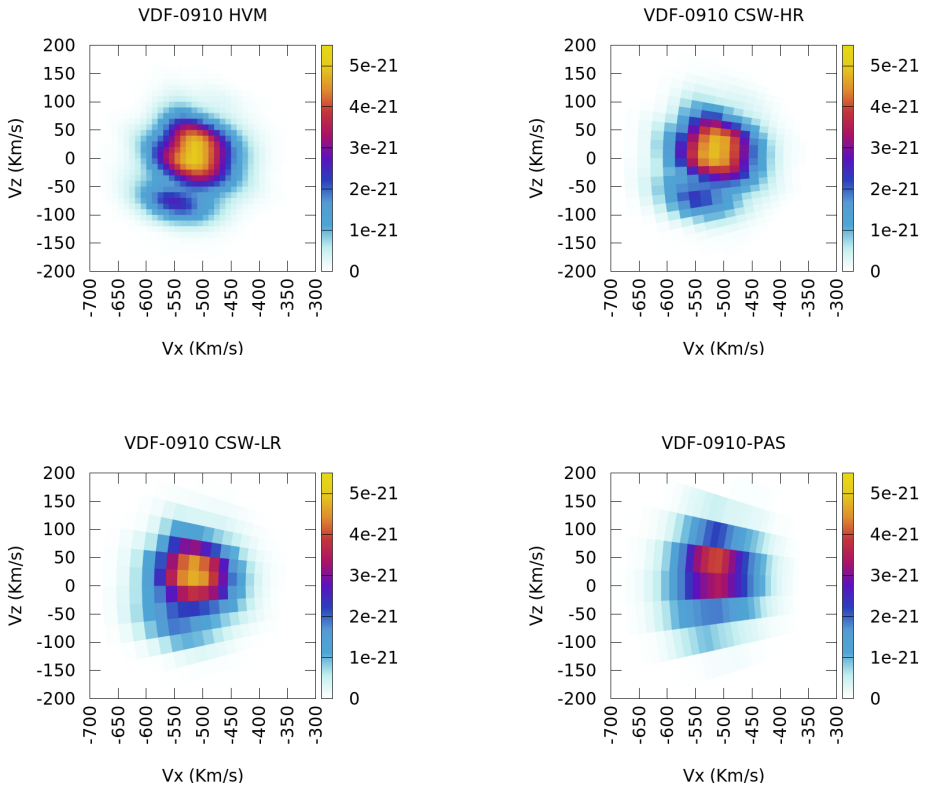

Figure 3. VDF # 2 (in $cm^{-6}s^3$) as it appears from the HVM simulation (top left), from the CSW simulations (top right and bottom left) and from PAS simulation.

5 Errors

To better express how the different sensors reproduce the actual VDFs we calculate the non-Maxwellianity indicator ϵ [11], given by:

$$\epsilon = \frac{1}{n}\sqrt{\int (f-g)^2 d^3v} \tag{5.1}$$

where n is the density, f is the "real" distribution function, coming either from HVM simulation and from the sensors, g is the isotropic Maxwellian calculated from the moments of f, i.e. (in Cartesian coordinates):

$$g = C\exp\left[\frac{1}{2T_{iso}}\sum_i (v_i - V_i)^2\right] \tag{5.2}$$

where V_i is computed from eq. (4.2) and $T_{iso} = (T_{\parallel} + T_{\perp 1} + T_{\perp 2})/3$. The quantity ϵ gives information about any departure from Maxwellian.

In figure 6 we report the quantity ϵ for the three simulated sensor and for the HVM code. As expected, the CSW-HR performs better in reproducing the details of the original VDFs.

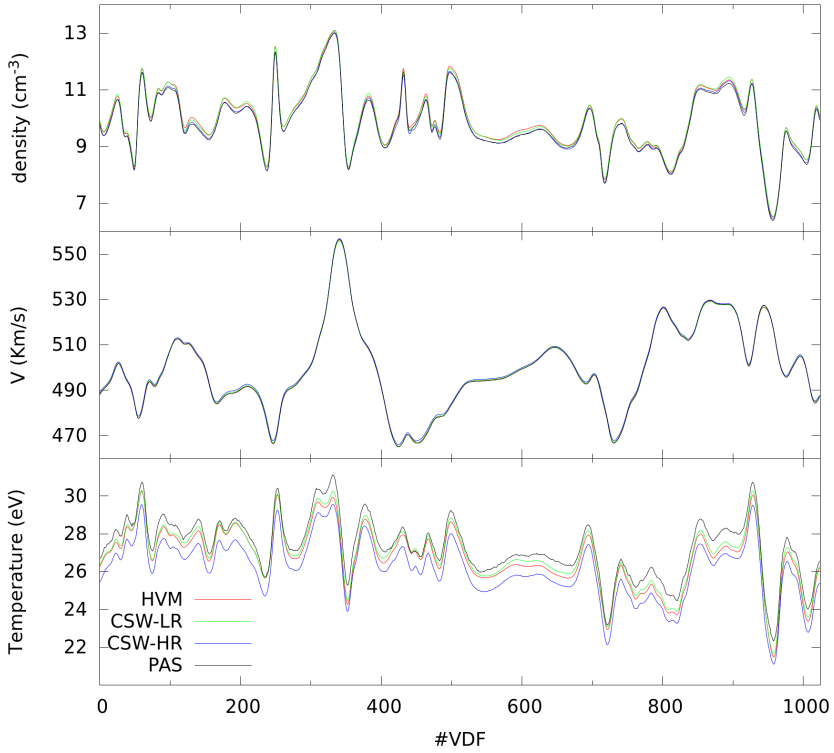

Figure 4. Density, total velocity and total temperature calculated from HVM simulation and for the simulated sensors for 1024 VDFs.

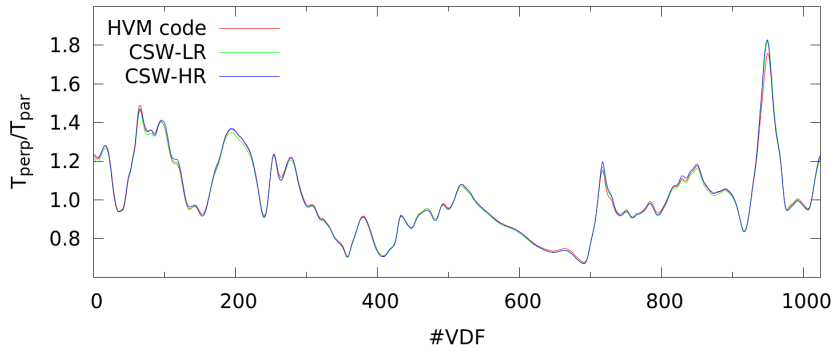

Figure 5. Temperature anisotropy calculated from HVM simulation and for the simulated sensors.

In order to give a quantitative evaluation of how the phase space resolution impacts on moments we calculate the average errors $\Delta n/n$, $\Delta V/V$, $\Delta T/T$, along with $\Delta\epsilon/\epsilon$ for PAS, CSW-HR and CSW-LR, where $\Delta n/n$ stands for $\frac{\sum |n_{sensor}-n_{HVM}|/n_{HVM}}{1024}$ and similarly for the other errors. In figure 7 the relative errors on moments in addition to the relative error on ϵ are reported. We see that, concerning moments, CSW-LR in general performs better than the other sensors, with results very similar to that of PAS, and CSW-HR is the best in rendering VDFs (little $\Delta\epsilon/\epsilon$). The good performance of CSW-LR is possibly due to a higher number of particles per energy/angle bin. Indeed, the relative uncertainty in an energy/angle bin is equal to $1/\sqrt{N}$ (N number of particles per bin) since counts

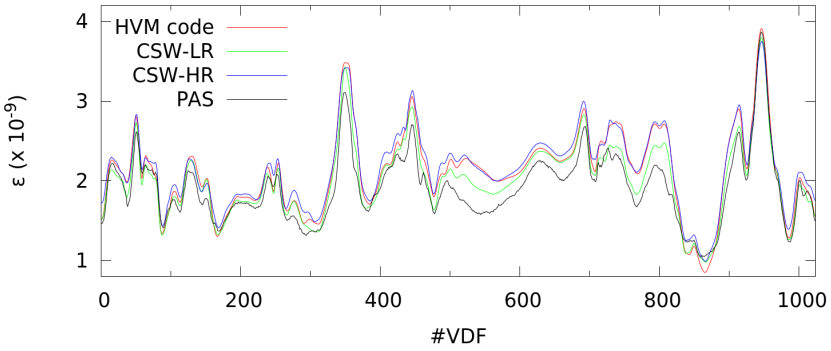

Figure 6. "Distance" from Maxwellian VDF calculated from HVM simulation and for the simulated sensors.

obey Poisson statistics. This uncertainty propagates to moments. CSW-HR, due to the smaller size of the angular sector and smaller accumulation time has a smaller counting statistics and thus a higher relative uncertainty. The same holds for PAS which has a smaller geometric factor and a smaller $\Delta E/E$. In order to investigate further the effect of the number of counts on relative errors, we tried to simulate CSW-HR with a higher geometric factor so that the number of counts per bin is increased. The results of the simulation (not shown here) indicate that all the errors on moments decrease with respect to the "real" CSW-HR. In particular, the moment which benefits more from a greater number of counts is the temperature, which presents smaller errors and it is no more regularly underestimated with respect to the HVM temperature.

Velocity has a small error in all the simulated instruments. This could be ascribed to the fact that, as reported in [14], while error on density scales as $1/\sqrt{N}$, error on velocity scales as $1/(M\sqrt{N})$ where M is the sonic Mach number, defined as the ratio between the bulk velocity and the thermal speed.

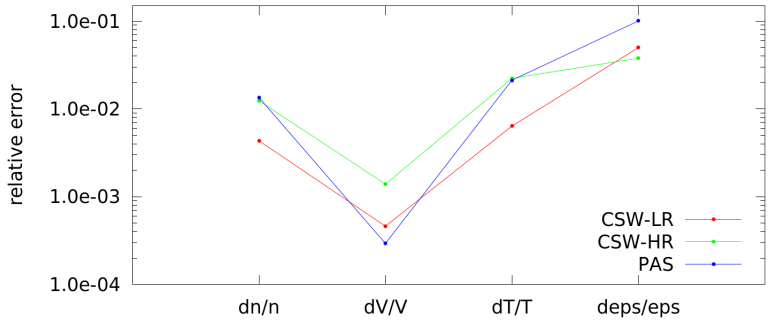

Figure 7. Relative errors for the simulated instruments

It has to be stated that the results above hold in the case of *ideal* instruments, where all the errors are due to the phase space resolution. Real measurements will be affected also by other instrumental effects, due to digitalization, degradation of detector efficiency and analyser voltages, out-of-energy counts, dead-time effects at high count rates and so on.

6 Summary and conclusions

Adequacy of energy/angular resolution of particle instruments is crucial to fully understand energy dissipation and particle energization processes. Hybrid Vlasov-Maxwell simulations provide small-scale proton VDFs in presence of solar-wind turbulence. We simulate how such VDFs are measured by the top-hat analysers dedicated to solar wind observation on SoLO and THOR. Our results show that kinetic features of VDFs are readily recognized only when angular resolution is below 5°; errors on moments and non-Maxwellianity indicators are generally lower for higher angular resolution, but low counting statistics could weaken the benefit of enhanced angular resolution. The present work confirms that PAS is well suited for solar wind turbulence studies and CSW will meet the more demanding scientific requirements of THOR.

Acknowledgments

This work has been supported by the Agenzia Spaziale Italiana under grants ASI-INAF 2015–039–R.O and ASI-INAF I/013/12/1. Work at IRAP was supported by CNRS and CNES.

References

[1] E. Sonnendrücker, J. Roche, P. Bertrand, and A. Ghizzo, *The Semi-Lagrangian Method for the Numerical Resolution of the Vlasov Equation*, *J. Comput. Phys.*, **149** (1999) 201.

[2] F. Valentini, P. Trávníček, F. Califano, P. Hellinger, and A. Mangeney, *A hybrid- Vlasov model based on the current advance method for the simulation of collisionless magnetized plasma, J. Comput. Phys.*, **225** (2007) 753.

[3] J. A. Araneda, Y. Maneva, and E. Marsch, *Preferential Heating and Acceleration of α Particles by Alfvén-Cyclotron Waves, Phys. Rev. Lett.*, **102** (2009) 175001.

[4] E. Camporeale and D. Burgess, *The Dissipation of Solar Wind Turbulent Fluctuations at Electron Scales, ApJ,* **730** (2011) 114.

[5] K. J. Bowers, B. J. Albright, L. Yin, W. Daughton, V. Roytershteyn, B. Bergen, and T. J. T. Kwan, *Advances in petascale kinetic plasma simulation with VPIC and Road-runner, Journal of Physics Conference Series,* **180** (2009) 012055.

[6] Stefano Markidis, Giovanni Lapenta, and Rizwan-uddin, *Multi-scale simulations of plasma with ipic3d. Mathematics and Computers in Simulation*, **80 (7)** (2010) 1509.

[7] Götz Paschamnn and Patrick W. Daly (Eds.), *Analysis Methods for Multi-spacecraft Data* Electronic Edition 1.1, ESA Publications Division (2000).

[8] E. Camporeale and D. Burgess, *The Dissipation of Solar Wind Turbulent Fluctuations at Electron Scales, ApJ,* **730** (2011) 114.

[9] H. Karimabadi, V. Roytershteyn, M. Wan, W. H. Matthaeus, W. Daughton, P. Wu, M. Shay, B. Loring, J. Borovsky, E. Leonardis, S. C. Chapman, and T. K. M. Nakamura, *Coherent structures, intermittent turbulence, and dissipation in high-temperature plasmas*, *Phys. Plasmas*, **20** (2013) 012303.

[10] S. Servidio, F. Valentini, F. Califano, and P. Veltri, *Local Kinetic Effects in Two-Dimensional Plasma Turbulence, Phys. Rev. Lett*, **108** (2012) 045001.

[11] F.Valentini, S. Servidio, D. Perrone, F. Califano, W. H. Matthaeus, and P. Veltri, *Hybrid Vlasov-Maxwell simulations of two-dimensional turbulence in plasmas*, *Phys. Plasmas*, **21** (2014) 082307.

[12] B. Lavraud, J. De Keyser, C. Amoros, E. Neef, M. Anciaux, N. Andre, R. Baruah, S. Berkenbosch, S. Bonnewijn, A. Cara, M. Echim, A. Fedorov, V. Genot, L. Licciardi, P. Louarn, J. Maes, R. Maggiolo, R. Mathon, S. Ranvier, and K.-W. Wong, *THOR Cold Solar Wind (CSW) instrument*, European Geophysical Union, Abstract EGU2016-7431, 2016.

[13] A. Cara, B. Lavraud, A. Fedorov, J. De Keyser, R. DeMarco, and M. F. Marcucci, F. Valentini, S. Servidio, *Electrostatic analyzer design for solar wind proton measurements with high temporal, energy, and angular resolutions*. Submitted to J. Geophys. Res.

[14] Daniel J. Gershman, John C. Dorelli, Adolfo F. Viñas, and Craig J. Pollock, *The calculation of moment uncertainties from velocity distribution functions with random errors, J. Geophys. Res. Space Physics*, **120**, 6633.